RSC Advances

ROYAL SOCIETY OF CHEMISTRY

www.rsc.org/advances

Journal Name

COMMUNICATION

NIR Luminescence for the Detection of Latent Fingerprints Based on ESIPT and AIE Processes†

Received 00th January 20xx,
Accepted 00th January 20xx

DOI: 10.1039/x0xx00000x

www.rsc.org/

Xiaodong Jin,[a] Libo Dong,[b] Xiaoyu Di,[a] Hai Huang,[a] Jingning Liu,[b] Xiaoli Sun,[c] Xueqiong Zhang,[a] and Hongjun Zhu*[a]

In this paper, a facile near infrared (NIR, 650-900 nm) probe 4-dimethylamino-2'-hydroxychalcone (NIR-LP) based on the excited state intramolecular proton transfer (ESIPT) - aggregation induced emission (AIE) processes for the detection of the latent fingerprints (LFPs) was developed for the first time. The probe can distinguish the fresh LFPs, but also recognize the aged (10 days) LFPs.

With contact between two items, there will always be an exchange. By applying Locard's exchange principle, the latent fingerprints (LFPs) can be identified well. Because of the uniqueness and permanence of the friction ridge arrangements, fingerprints have been used as a means to biometrically identify individuals in forensic investigations since the late 19th century.[1] To date, it is also widely used in individual credentials, access control, safety inspection and other fields. However, the most commonly found fingermarks are typically latent (termed latent fingerprints), and require "development" to permit their visualization.[2] Thus, the detection and identification of the LFPs is an indispensable strategy in individual credential and forensic science.[3] Commonly, The LFPs is usually developed using methods such as powder (metallic, magnetic, or fluorescent powder) dusting,[4] chemical fumes (iodine fuming, cyanoacrylate fuming)[5] and multi-metal deposition method (MMD). However, these traditional techniques are inevitably associated with serious problems in developing latent fingermarks, such as high toxicity, low detection sensitivity, and high background interference.

Numerous efforts have been made in recent years to improve the existing techniques for better visualization of the LFPs, especially the use of quantum dots (QDs),[6] electrochemistry (ECL)[7,8], immunological multimetal deposition (iMMD)[2] and mass spectrometry.[9] However, some of these methods require heavy instrumentation, complex procedures, environmental unfriendly or expensive materials, and materials with less sensitivity. Therefore, to develop a simple and sensitive new techniques for better LFP imaging is of great importance.

To our delight, an elegant solution has been recently presented in two reports by Su's research group.[10,11] They first proposed a novel use of the aggregation induced emission (AIE) effect of the dyes, such as tetraphenylethene (**TPE**), 1,1,2,3,4,5-hexaphenylsilole (**HPS**) and 1-methyl-1-(4-carboxystyrene)-2,3,4,5-tetraphenylsilole (**MCSTPS**) for the visualization enhancement of LFPs on wet non-porous surfaces (Fig 1). Practically, the wet chemistry treatment on one hand may protect policemen from the harmful effects of dust. On the other hand, AIE-active luminogens outshine their aggregation-caused quenching (ACQ)-counterparts in many applications and overcome problems previously associated with ACQ luminogens in which the emission of these ACQ luminogens is attenuated at high concentrations or in the solid state. Therefore, by employing AIE strategy, the ACQ effect can be well avoided and displayed under a low background interference when the LFPs is detected. However, it can't deny that these AIE molecules mentioned above do have a UV radiation and complicated synthetic processes. Considering the limited number and drawbacks of the existing AIE fluorescent probes for the LFPs, facile NIR fluorescent sensors for a rapid highly-sensitive detection of the LFPs are therefore still expected to be developed.

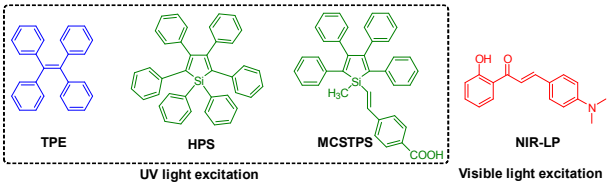

Fig. 1 Molecular structures of **TPE**, **HPS**, **MCSTPS** and **NIR-LP**.

[a] Department of Applied Chemistry, Nanjing Tech University, Nanjing, Jiangsu, 211816, P. R. China. E-mail: zhuhj@njtech.edu.cn
[b] Department of Criminal Science and Technology, Jiangsu Police Institute, Nanjing, Jiangsu, 210031, P. R. China.
[c] Jiangsu Key Laboratory for Molecular and Medical Biotechnology, Nanjing Normal University, Nanjing, Jiangsu, 210032, P. R. China.
† Footnotes relating to the title and/or authors should appear here.
Electronic Supplementary Information (ESI) available: [details of any supplementary information available should be included here]. See DOI: 10.1039/x0xx00000x

According to the relevant literatures,[12, 13] a sensor with far-red or near infrared (NIR, 650-900 nm) emission is with low photo toxicity and under low auto-fluorescent background, making it friendly to human body. Herein, in this paper, we explore the possibility of identifying LFPs on the basic of a novel AIE probe **4-dimethylamino-2'-hydroxychalcone (NIR-LP)**. Compared with the above three AIE molecules (Fig. 1) emitting blue color, the sensor **NIR-LP** has a visible-light-excitable wavelength and NIR emission, which helps to lower the background fluorescence. Therefore, to design a fluorescent probe with red emission for the LFPs identification is desired. Moreover, the probe can not only distinguish the fresh LFPs, but also recognize the aged (10 days) LFPs.

The chemosensors (**NIR-LP**) was prepared by the reported method.[14] **NIR-LP** is synthesized with 2'-hydroxyacetophenone and 4-dimethylaminobenzaldehyde through Claisen-Schmidt condensation reaction under mild basic conditions with only one step (scheme 1). It is worth noting that the synthetic procedure for the probe **NIR-LP** is simple, as no column chromatography is required in the process of purification. The structure of **NIR-LP** was confirmed by NMR. (see ESI†, Figs.S1-S2)

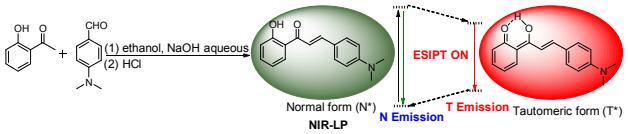

Scheme 1. The routes of synthesis of compound **NIR-LP**.

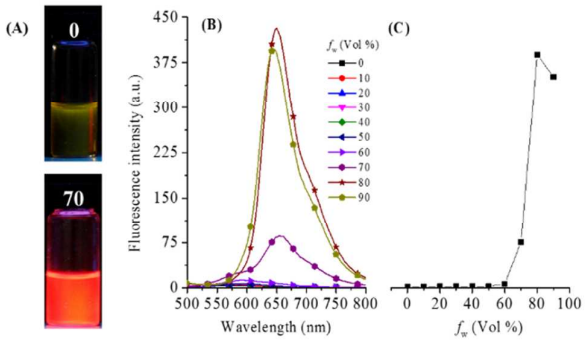

Fig. 2 (a) Photographic images of **NIR-LP** dissolved in water and in the CH_3CN–water mixture (water volume fraction, f_w = 70) under illumination by a UV lamp at 365 nm. (b) Emission spectra of NIR-LP in CH_3CN and CH_3CN-water mixture with different f_w. **NIR-LP** concentration: 0.25 mM, λ_{ex} = 430 nm. (c) Plot of emission peak intensity against f_w. **Note:** Spectral data were recorded 20 min after the addition of water to the CH_3CN solvent.

NIR-LP is a new AIE-active which has been reported by Tang's group recently.[15] The molecule undergoes the excited state intramolecular proton transfer (ESIPT) process through enol form to keto form and generates a well conjugated structure with alternating single and double bonds thus inducing redder emission.[15, 16] It is weak fluorescent (N*, normal form) when dissolved in good solvents (e.g. acetonitrile, ethanol, and THF), but becomes strongly emissive in poor solvents (e.g. water). This is probably that the **NIR-LP** molecules are excited under fluorescent illumination and ESIPT occurs, and thus generates resonance structures or isomerization (shown in scheme 1). As shown in Scheme 1 and Fig. 2A, when a small amount of poor solvent water is added into the CH_3CN solution, the intramolecular hydrogen bonding is impaired, and the ESIPT process is inhibited. Therefore, the mixture starts to emit a greenish-yellow emission (N*, normal form). However, when the water volume fraction (V:V) was beyond 70%, the sensor **NIR-LP** easily forms nanoparticle in aqueous media due to its poor water solubility and reforms the intramolecular hydrogen bonding in **NIR-LP**, and the ESIPT process brings the keto form (T*, tautomeric form) of **NIR-LP** to emit red fluorescence intensively (Fig. 2B and C). As a result, the nanoparticle of **NIR-LP** will activate the AIE and ESIPT processes. However, when the water fraction reaches 90%, a large amount of block deposit is precipitated and floated on the liquid surface, thereby decreasing the solution emission. As reported previously, the molecular conformation is responsible for the AIE effect.[15]

The sebum-rich fingerprint development procedure is fairly simple. Before fingerprint samples were collected, volunteers should be cleaned up their fingers with soap. Subsequently, they gently rubbed their fingertips over the forehead or nose and stamping them on different substrates (including aluminium foils, coins and glass slides) to leave fingermarks that contain sebaceous materials (sebum). The substrate was swayed for an appropriate period of time (20 min) in the CH_3CN-water mixtures of **NIR-LP** with different amounts of water, then gently rinsed with water twice or thrice. The fluorescence image of the LFPs arose under ultraviolet light illumination at 365 nm, and a photograph was recorded with a common digital camera.[17]

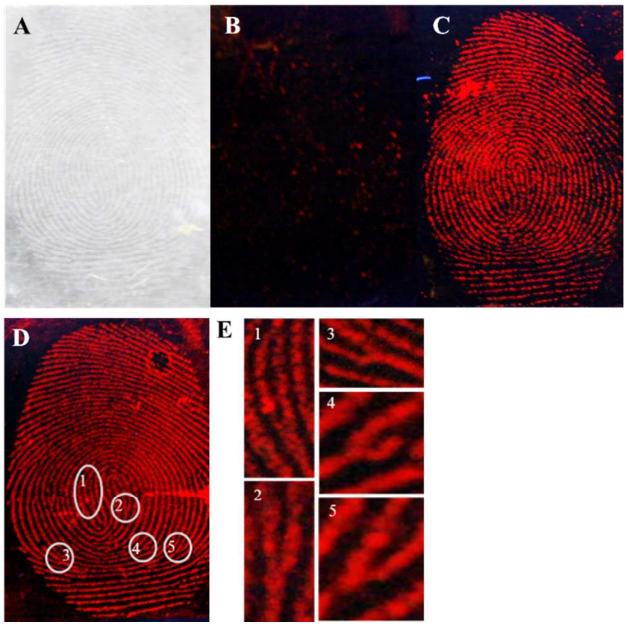

Fig. 3 (A) Images of fresh sebaceous fingerprints on a aluminium foil with sebaceous fingerprint but no **NIR-LP**. Fluorescent image of

sebaceous fingerprint on a aluminum foil developed by AIE of **NIR-LP** aggregates. **NIR-LP** concentration: 0.25 mM, the water fraction was 60% (B), 70% (C) and 80% (D), respectively. (E) Fluorescence images of LFPs showing level 2 details including lake (1) and bifurcation (2, 3, 4, 5). All fluorescent images were excited with a 365 nm UV lamp.

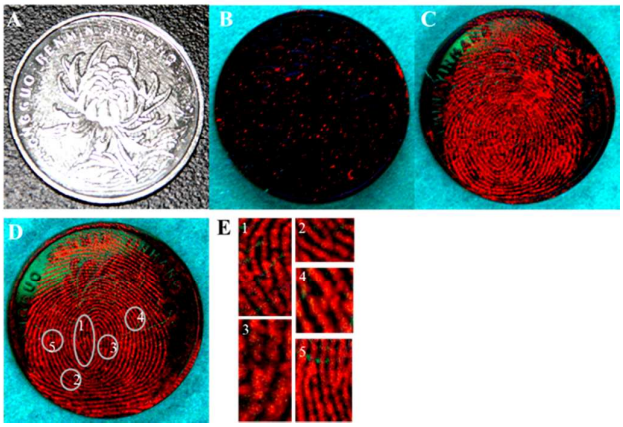

Fig. 4 (A) Images of fresh sebaceous fingerprints on a coin with sebaceous fingerprint but no **NIR-LP**. Fluorescent image of sebaceous fingerprint on a coin developed by AIE of **NIR-LP** aggregates. **NIR-LP** concentration: 0.25 mM, the water fraction was 60% (B), 70% (C) and 80% (D), respectively. (E) Fluorescence images of LFPs showing level 2 details including lake (1), bifurcation (2, 3, 5) and island (4). All fluorescent images were excited with a 365 nm UV lamp.

Due to the excellent optical and AIE properties of the sensor **NIR-LP**, we intended to explore the application of the sensor **NIR-LP** for potential LFPs imaging. As we all know that the substructures[18,19] (three different levels, namely, level 1 (pattern), level 2 (minutia points), and level 3 (pores and ridge contours)) of LFPs in principle form the basis of fingerprint identification, and their unambiguous imaging is critical for forensic identification of individuals. Our results show that a fresh latent fingerprint deposited on different substrate surfaces, such as aluminium foils (Fig.3), coins (Fig.4) and glass slides (Fig.5), could be clearly seen (Fig.3C and D, Fig.4C and D, Fig.5C and D) when excited with a 365 nm UV lamp, with ridges, furrows, and other details clearly visible.

However, the LFPs are barely visible under daylight (Figs. 3A, 4A and 5A). The sebum-rich fingerprint staining with the sensor **NIR-LP** (Figs. 3D, 4D and 5D) displays a well-resolved ridge flow and pattern configuration (level 1). In addition to level 1 details, level 2 (ridge termination, bifurcation, lake, island and crossover) characteristics of the LFPs are also clearly observed (Figs. 3D, 4D and 5D), suggesting strong interactions between the sensor **NIR-LP** nanoparticles and eccrine excretions. It is noted that we can not get the enhanced fluorescent LFPs images at or below f_w = 60 (Figs. 3B, 4B and 5B), which is assumed that the ESIPT process in the sensor **NIR-LP** might not be reformed at or below f_w = 60 (Fig. 2B). Moreover, the LFPs images (Fig. 6) obtained by the sensor **NIR-LP** were generally the same (from the same volunteer) because the macro details such as pattern type, singular points and friction ridge flow of the three images are similar. Additionally, a series of similar minutia points of the three images can be found (16 of which are labelled in Fig. 6), confirming the accuracy of using the sensor for LFPs detection. It should be noted that the amount of characteristics varies from one another, and is usually between 8 and 16 matches.[20]

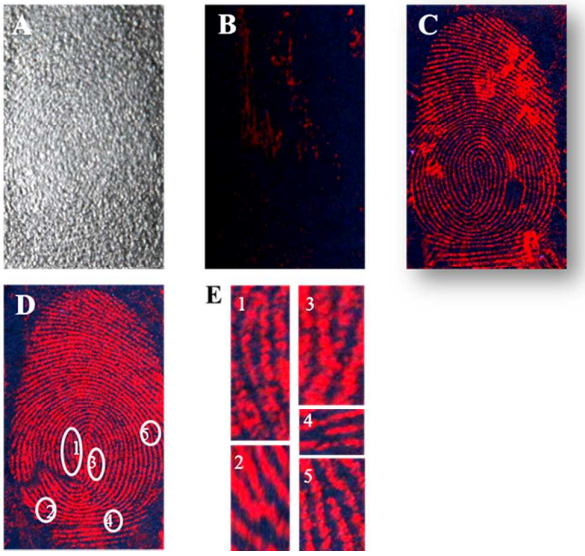

Fig. 5 (A) Images of fresh sebaceous fingerprints on a glass with sebaceous fingerprint but no **NIR-LP**. Fluorescent image of sebaceous fingerprint on a glass developed by AIE of **NIR-LP** aggregates. **NIR-LP** concentration: 0.25 mM, the water fraction was 60% (B), 70% (C) and 80% (D), respectively. (E) Fluorescence images of LFPs showing level 2 details including lake (1), bifurcation (2, 3) and termination (4, 5). All fluorescent images were excited with a 365 nm UV lamp.

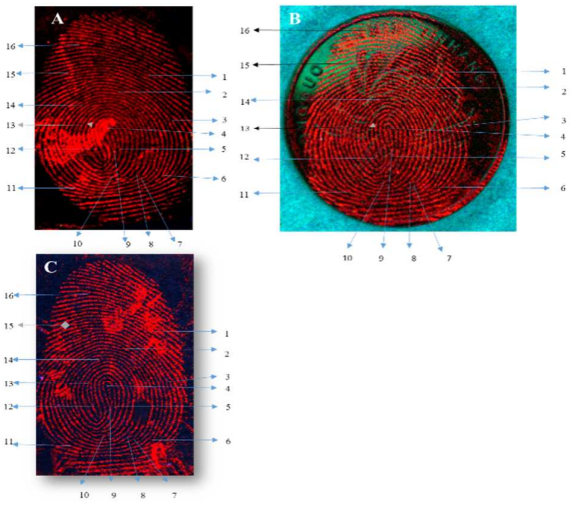

Fig. 6 Fingerprint detection by **NIR-LP**, irradiated by UV light onto the surface of an aluminium foil (A), coin (B), and glass slide (C) analysis of correspondences.

In real crime scenes, we are more likely to encounter aged fingerprint. Thus we further demonstrate the robustness of the sensor for practical use, and aged fingerprints (10 days) were developed. As shown in Fig. 7, the fingerprint ridge details could still be well visualized.

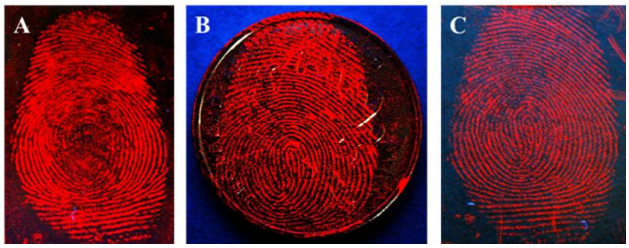

Fig. 7 Images of old sebaceous fingerprints on a aluminium foil (A), coin (B) and glass (C) developed by AIE of **NIR-LP** aggregates. **NIR-LP** concentration: 0.25 mM, the water fraction was 80%. All fluorescent images were excited with a 365 nm UV lamp.

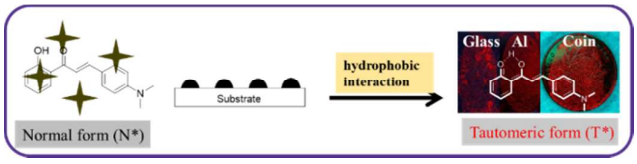

Scheme 2. The proposed mechanism of the fingerprint enhancement by AIE of **NIR-LP**.

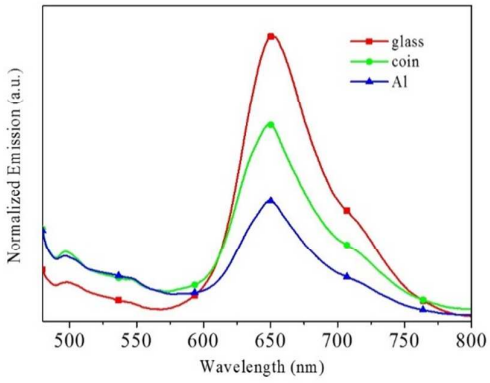

Fig. 8 Emission spectra of fingerprints on different substrate surfaces developed by **NIR-LP** nanoparticles.

As reported previously,[10,11,21] hydrophobic particles preferentially adhere to the fatty residues of the latent fingerprints (Scheme 2). This leads to the deposition of AIE luminogens on the ridges and a sufficiently strong fluorescence contrast between the fingerprint and the substrate. From Fig. 3 to Fig. 7, it is indicated that the **NIR-LP** nanoparticles adhere preferentially to the fingerprint ridges and the ESIPT process is reformed, thus producing a fluorescence-enhanced LFPs image. The adsorption of **NIR-LP** crystals on the fingerprints was proved by solid state fluorescent emission, as shown in Fig. 8, which is in agreement with that observed in water-CH_3CN mixtures (Fig. 2B).

Conclusions

In summary, we have presented the synthesis and properties of a facile NIR sensor **NIR-LP** for the recognition of the latent fingerprints. Compared with the existing methods to identify the LFPs (Table S1), the probe **NIR-LP** is the first example of a NIR sensor possessing ESIPT - AIE property to visualize the latent LFPs in solution. In addition, this approach requires moderate incubation time (20 min) and needs no expensive or hazardous reagents, sophisticated instrument or post-treatment procedures. It is worth mentioning that we have successfully taken advantage of the probe **NIR-LP** to identify the old (10 days) latent fingerprint. This method employing fluorescent AIE materials is expected to be a quite simple, convenient, and universal technique for the high visualization of LFPs. We envisage that this AIE strategy can be used for various forensic applications.

Acknowledgements

This work is sponsored by the Science and Technology of Public Security of Jiangsu Police Institute - the Key Construction Disciplines at the Provincial Level of Jiangsu Province during 12th Five-Year Plan (2011-2015).

Notes and references

1 H. Chen, K. Chang, X. Men, K. Sun, X. Fang, C. Ma, Y. Zhao, S. Yin, W. Qin and C. Wu, *ACS Appl. Mater. Interfaces*, 2015, **7**, 14477-14484.
2 Y. He, L. Xu, Y. Zhu, Q. Wei, M. Zhang and B. Su, *Angew. Chem., Int. Ed.*, 2014, **53**, 12609-12612.
3 S. Bell, *Annual Review of Analytical Chemistry*, 2009, **2**, 297-319.
4 G. S. Sodhi and J. Kaur, *Forensic Sci. Int.*, 2001, **120**, 172-176.
5 T. C. Fung, K. Grimwood, R. Shimmon, X. Spindler, P. Maynard, C. Lennard and C. Roux, *Forensic Sci. Int.*, 2011, **212**, 143-149.
6 C. Xu, R. Zhou, W. He, L. Wu, P. Wu and X. Hou, *Anal. Chem.*, 2014, **86**, 3279-3283.
7 L. Xu, Y. Li, S. Wu, X. Liu and B. Su, *Angew. Chem.*, 2012, **124**, 8192-8196.
8 L. Xu, Z. Zhou, C. Zhang, Y. He and B. Su, *Chem. Commun.*, 2014, **50**, 9097-9100.
9 J. Sekuła, J. Nizioł, W. Rode and T. Ruman, *Anal. Chim. Acta.*, 2015, **875**, 61-72.
10 Y. Li, L. Xu and B. Su, *Chem. Commun.*, 2012, **48**, 4109-4111.
11 L. Xu, Y. Li, S. Li, R. Hu, A. Qin, B. Z. Tang and B. Su, *Analyst*, 2014, **139**, 2332-2335.
12 D. Yu, F. Huang, S. Ding and G. Feng, *Anal. Chem.*, 2014, **86**, 8835-8841.
13 S. Chen, P. Hou, B. Zhou, X. Song, J. Wu, H. Zhang and J. W. Foley, *RSC Advances*, 2013, **3**, 11543-11546.

14 Y. Liu, D. Yu, S. Ding, Q. Xiao, J. Guo and G. Feng, *ACS Appl. Mater. Interfaces*, 2014, **6**, 17543-17550.
15 Z. Song, R. T. K. Kwok, E. Zhao, Z. He, Y. Hong, J. W. Y. Lam, B. Liu and B. Z. Tang, *ACS Appl. Mater. Interfaces*, 2014, **6**, 17245-17254.
16 T. Teshima, M. Takeishi and T. Arai, *New J. Chem.*, 2009, **33**, 1393-1401.
17 F. Wang, J. Chen, H. Zhou, W. Li, Q. Zhang and C. Yu, *Anal. Methods*, 2014, **6**, 654-657.
18 R. M. Sapstead Nee Brown, K. S. Ryder, C. Fullarton, M. Skoda, R. M. Dalgliesh, E. B. Watkins, C. Beebee, R. Barker, A. Glidle and A. R. Hillman, *Faraday Discuss.*, 2013, **164**, 391-410.
19 K. Li, W. Qin, F. Li, X. Zhao, B. Jiang, K. Wang, S. Deng, C. Fan and D. Li, *Angew. Chem., Int. Ed.*, 2013, **52**, 11542-11545.
20 M. Algarra, K. Radotić, A. Kalauzi, D. Mutavdžić, A. Savić, J. Jiménez-Jiménez, E. Rodríguez-Castellón, J. C. G. E. Silva and J. J. Guerrero-González, *Anal. Chim. Acta.*, 2014, **812**, 228-235.
21 M. Sametband, I. Shweky, U. Banin, D. Mandler and J. Almog, *Chem. Commun.*, 2007, 1142-1144.